

DEVELOPMENT OF AERODYNAMIC DESIGN PROCESS FOR REUSABLE WINGED SPACE VEHICLE USING OPENVSP

Saori Taishi
Tokyo Metropolitan University
6-6 Asahigaoka Hino Tokyo Japan

Keywords: *Global design optimization, OpenVSP, Winged space vehicle*

Abstract

In this study, a vehicle design procedure is developed using NASA's Open Vehicle Sketch Pad (OpenVSP), which is a parametric aircraft/spacecraft geometry definition tool. A model defined by OpenVSP can be directly used for analysis with computational fluid dynamics (CFD). Model data for OpenVSP are constructed using extensible markup language (XML), which can be considered as a layered structure. Using this feature, the design procedure can change not only the geometry, but also the topology of a design. The procedure that includes OpenVSP can reduce the cost of the conceptual design phase and a high-fidelity analysis can be performed. In this study, a design procedure based on OpenVSP and a high-fidelity flow solver is proposed. The procedure is applied to the design of the winged space transport vehicle. The design variables are the cant and sweep angles of the vertical tail, with the aim of achieving better stability in the landing phase. Using this design procedure, the knowledge of the design space can be acquired efficiently, such as the resulting variance of the lift and pitching moment.

1 Introduction

Novel concepts for space transportation should consider operational cost with the aim of improving efficiency. There are many different types of space vehicles that are currently under development. The winged space vehicle is a candidate for the next generation of efficient spacecrafts, because this type of space vehicle

has the advantage of being able to land on runways at conventional airports.

In order to optimize an airframe for a reentry vehicle, many simulation cases need to be calculated. This is because many flight conditions must be considered in the design phase, such as subsonic, transonic, supersonic, and hypersonic (Fig. 1). Therefore, the design method should be able to explore the design space widely. Open Vehicle Sketch Pad (OpenVSP)^[1] is a software tool developed by NASA that has many types of pre-defined components, such as the wing, fuselage, and engine. It is an efficient tool for aircraft/spacecraft definition, because the shape of each component and the topology of the vehicle can be considered at the same time. OpenVSP can express the shape of a design as a layered data structure by using the extensible markup language (XML). Therefore, geometry and topology can be controlled globally by editing the expressions of each layer. This study investigates the efficiency of the proposed design procedure for a winged spacecraft, using a framework with OpenVSP as an efficient global representation tool.

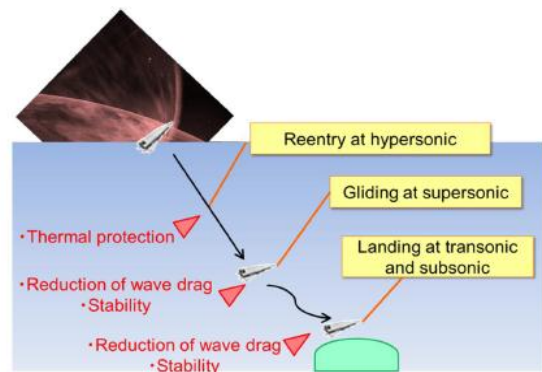


Fig. 1 Reentry vehicle and multiphase design

2 Design Suggestions

A design procedure is developed, employing OpenVSP as a geometry representation tool. For flow computation, we apply an unstructured mesh generator, Hexagrid^[2], and the compressible flow solver FAST Aerodynamic Routines (FaSTAR)^[3].

2.1 Geometry Representation using Open VSP

OpenVSP is a design tool that can be used for creating the conceptual design of an aircraft. OpenVSP can be used for the efficient and rapid definition of aerodynamic geometry with a few steps. In general, a designer selects fundamental components, such as fuselages, multi-section wings (MS_Wing), and engines from the list of templates in OpenVSP. Each component can be designed in detail by defining parameters. A designer can define a new component that is not listed in OpenVSP using a basic component such as a fuselage. For example, an engine nozzle can be represented by a modified fuselage component. The beneficial feature of OpenVSP is that geometry data are written in XML, which can be considered as a layered structure, as shown Fig. 2. Using this feature, the design procedure includes not only the geometrical but also the topological design. Thus, the use of OpenVSP can simplify the design steps, as shown in Fig. 3. OpenVSP can be operated through both the graphical user interface (GUI) and the character user interface (CUI).

2.2 Grid Generation

Hexagrid is a hexahedral element grid generator that is used in this study, and was developed at Japan Aerospace Exploration Agency (JAXA). It automatically generates a hexahedral grid around a solid surface, requiring only the maximum and minimum grid size, and the minimum size of the prism layer for calculating the boundary layer flow. It is suitable for generating a computational mesh around a complex aircraft design. A beneficial feature of Hexagrid is that it can perform batch

generation of meshes for more than one Stereolith (.stl) file produced by OpenVSP.

2.3 Flow Solver

FaSTAR is employed as the flow solver for an unstructured mesh. It can be used for compressible Reynolds-averaged Navier-Stokes simulations (RANS). FaSTAR is optimized for short-time simulations with computational meshes produced by Hexagrid, and several subroutines are modularized. The convergence can be improved by using a multi-grid method. FaSTAR is constructed from pre-process, solver, and post-process parts. The pre-process part has many techniques to improve the quality of a poor input mesh.

This study uses the compressible Navier-Stokes equations (1–3). Q is a conservative quantity in a control volume, and F is the flux of the conservative quantity that flows in or out of the control volume.

In this study, simple low-dissipation AUSM (SLAU) is used for the inviscid flux evaluation, and time integration is performed by the lower/upper symmetric Gauss-Siedel method (LU-SGS). The Spalart-Allmaras (SA) turbulence model is also used.

$$\frac{\partial}{\partial t} \int_{\Omega} Q dv + \oint_{\partial\Omega} F \cdot nds = 0 \quad (1)$$

$$Q = \begin{bmatrix} \rho \\ \rho u \\ \rho v \\ \rho w \\ e \end{bmatrix} \quad (2)$$

$$F = \begin{bmatrix} \rho u \\ p + \rho u^2 - \tau_{xx} \\ \rho uv - \tau_{xy} \\ \rho uw - \tau_{xz} \\ (e + p)u - \tau_{xx}u - \tau_{xy}v - \tau_{xz}w - \kappa T_x \end{bmatrix} + \begin{bmatrix} \rho v \\ \rho uv - \tau_{yx} \\ p + \rho v^2 - \tau_{yy} \\ \rho vw - \tau_{yz} \\ (e + p)v - \tau_{yx}u - \tau_{yy}v - \tau_{yz}w - \kappa T_y \end{bmatrix} + \begin{bmatrix} \rho w \\ \rho vw - \tau_{zx} \\ \rho wv - \tau_{zy} \\ p + \rho w^2 - \tau_{zz} \\ (e + p)w - \tau_{zx}u - \tau_{zy}v - \tau_{zz}w - \kappa T_z \end{bmatrix} \quad (3)$$

2.4 Kriging Model

To reduce computational cost, this study uses Kriging interpolation^[4], which expresses the value of $y(x_i)$ at an unknown design point x_i as

$$y(x_i) = \mu + \varepsilon(x_i) \quad (i = 1, 2, \dots, m) \quad (4)$$

where m is the number of design valuables, μ is a constant global model, and $\varepsilon(x_i)$ represents a local deviation from the global model. The correlation between $\varepsilon(x_i)$ and $\varepsilon(x_j)$ is strongly related to the distance between x_i and x_j . In the proposed model, the local deviation at an unknown point x is expressed as a stochastic process. Some sample points are chosen, the relevant design data is calculated at these points, and then, they are interpolated using a Gaussian correlation function in order to estimate the trend of the stochastic process.

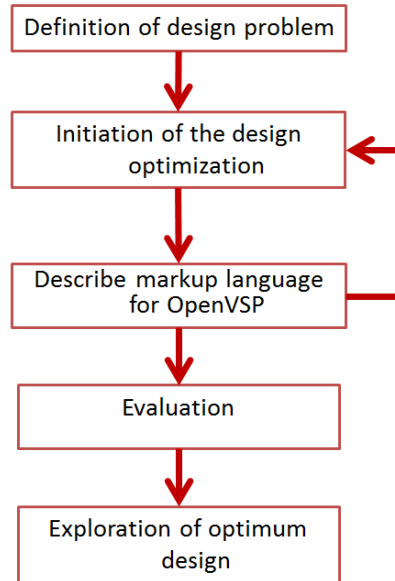


Fig. 3 Flow chart of the design method.

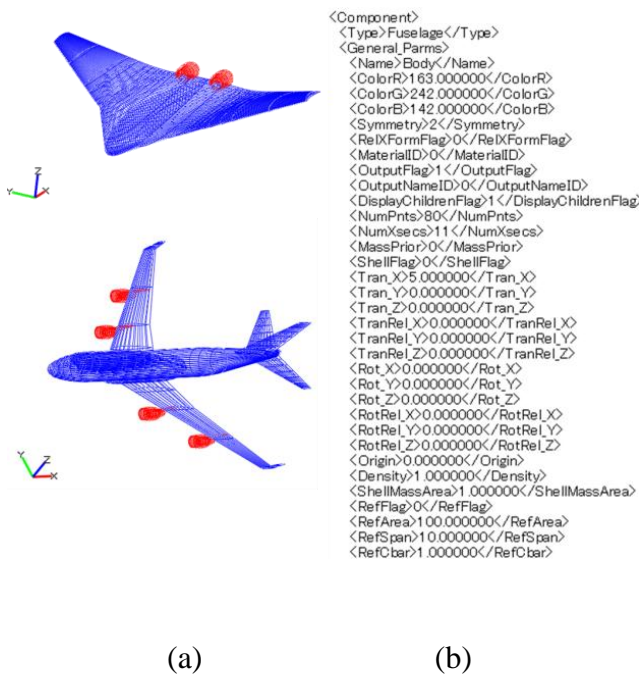


Fig. 2 Design example using OpenVSP.
(a) Geometries from OpenVSP.
(b) Example of geometrical data.

3 Initial Design

The baseline model is designed by OpenVSP and illustrated in Fig. 4. This concept is referred to as a “Reference system”^[5] design in JAXA. This vehicle would transport eight persons to a low Earth orbit. The total length is approximately 22 m. The lifting-body shape not only generates a lift but also provides a large interior volume relative to the size of the vehicle.

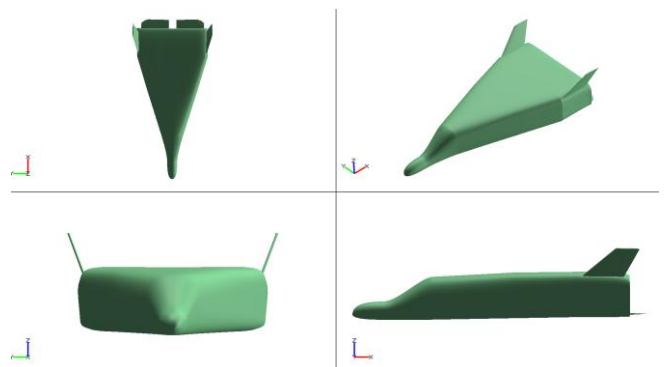


Fig. 4 Three-view of the initial design.

4 Results

One of the major advantages of a winged spacecraft is the ability to land on conventional runways at existing airports. To land at low speed, it is necessary to maintain stability. Therefore, this study focuses on the geometrical design of the vertical tail (V-tail), as an initial test of the proposed design procedure. Maximization of the lift is considered with respect to the trim balance. The landing conditions for the computation are listed in Table 1.

4.1 Geometry Representation using OpenVSP

The cant angle and sweep angle of the V-tail are shown in Fig. 5. Latin hypercube sampling (LHS)^[6] is employed for the design of experiments (DOE). Six pairs of angles are obtained by LHS and listed in Table 2.

The 3D design data are generated after updating only two parameters of the OpenVSP XML data, as shown in Fig. 6. The parameter for the cant angle is highlighted in red and the parameter for the sweep angle is highlighted in green.

4.2 Evaluation of Sample Designs

The resulting relationships between lift coefficient C_L and pitching moment coefficient C_M are shown in Fig. 7. This shows that designs #4 and #5 have the highest C_L at zero C_M . Because designs #4 and #5 have a large cant angle and sweep angle that can gain higher suction as shown in Fig. 8(b, c), it is reasonable that these designs will achieve the highest C_L . A design with a large cant angle achieves good performance; however, such a design can be expected to suffer from poor heat-resistance.

The initial design achieves a higher C_L than some of the sample designs, despite a low cant angle. Conversely, design #6 is considerably similar to the initial design, but cannot achieve a high C_L . These designs should offer good heat resistance, but the design variables are effective for maintaining the trim balance. Thus, we observe that the designs that have a small cant

angle are very sensitive to the input parameters and have to be designed carefully.

4.3 Visualization of Design Problem

Table 5 lists the estimated values of C_L (to be maximized) at $C_M=0$ from Fig. 7. The design problem is visualized by Kriging surrogate model as shown in Fig. 9. With reference to this figure, we seek the design with the highest C_L , that is the design that can bring back the heaviest payload to the ground. However, a large cant angle has a disadvantage in view of the design of the thermal protection system.

On the other hand, a design with a small cant angle also achieves a high C_L when the sweep angle is large. It is notable for designers that the design C_L becomes lower when the sweep angle becomes smaller.

By using this visualization, a designer is able to select an appropriate V-tail design. Namely, if the technical level of the thermal protection system is good, then a design with a larger cant angle can be selected. If the issue of thermal protection is severe, then a lower cant angle can also be selected, with optimization of the sweep angle. In addition, the results also suggest that the design still has possibility to achieve better performance without a V-tail, because the result suggests that the design with low cant angle has still possibility to be better design.

Thus, the design which does not have V-tail is considered. As shown in Fig. 10, the side wall of the fuselage is cutted out 20° , and the tail of the fuselage is also cut 50° with considering the equivalent low speed performance to the second peak (the cant angle is 20° , and the sweep back angle is 50°) of Fig. 9. Modified design are illustrated in Fig. 10.

Table 1 Computational conditions.

Mach number	0.3
Angle of attack	5, 10 and 15°
Reynolds number	1.21×10^7

DEVELOPMENT OF AERODYNAMIC DESIGN PROCESS FOR REUSABLE WINGED SPACE VEHICLE USING OPENVSP

Table 2 Sample V-tail design angles.

	Cant angle [deg.] (20-50)	Sweep angle [deg.] (39-59)
Initial design	20.0	49.0
Design #1	32.8	48.0
Design #2	41.0	45.2
Design #3	35.8	57.5
Design #4	49.3	54.6
Design #5	45.5	55.9
Design #6	24.6	44.9

Table 3 Estimated C_L at $C_M=0$.

	C_L
Initial design	0.158981
Design #1	0.151158
Design #2	0.155382
Design #3	0.153421
Design #4	0.162034
Design #5	0.159959
Design #6	0.144652

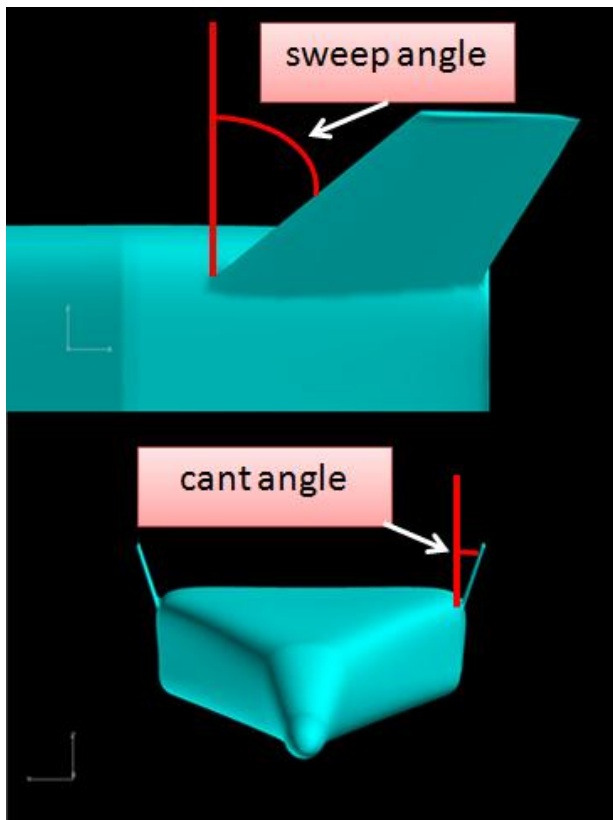


Fig. 5 Side and front views of base model with design points

```

<Name>Vtail</Name>
  <ColorR>0.000000</ColorR>
  <ColorG>0.000000</ColorG>
  <ColorB>255.000000</ColorB>
  <Symmetry>2</Symmetry>
  <RelXFormFlag>0</RelXFormFlag>
  <MaterialID>15</MaterialID>
  <OutputFlag>1</OutputFlag>
  <OutputNameID>0</OutputNameID>
  <DisplayChildrenFlag>1</DisplayChildrenFlag>
  <NumPnts>57</NumPnts>
  <NumXsecs>11</NumXsecs>
  <MassPrior>0</MassPrior>
  <ShellFlag>0</ShellFlag>
  <Tran_X>15.671442</Tran_X>
  <Tran_Y>4.261905</Tran_Y>
  <Tran_Z>1.550000</Tran_Z>
  <TranRel_X>0.000000</TranRel_X>
  <TranRel_Y>0.000000</TranRel_Y>
  <TranRel_Z>0.000000</TranRel_Z>
  <Rot_X>70.000000</Rot_X>
  <Rot_Y>0.535704</Rot_Y>
  <Rot_Z>0.000000</Rot_Z>
  <RotRel_X>0.000000</RotRel_X>
  <RotRel_Y>0.000000</RotRel_Y>
  <RotRel_Z>0.000000</RotRel_Z>
  <Origin>0.012500</Origin>
  <Density>1.000000</Density>
  <ShellMassArea>1.000000</ShellMassArea>
  <RefFlag>0</RefFlag>
  <RefArea>100.000000</RefArea>
  <RefSpan>10.000000</RefSpan>
  <RefCbar>1.000000</RefCbar>
</Airfoil_List>
<Section_List>
  <Section>
    <Driver>4</Driver>
    <AR>0.873562</AR>
    <TR>0.576471</TR>
    <Area>4.640035</Area>
    <Span>2.013295</Span>
    <TC>1.685525</TC>
    <RC>2.923869</RC>
    <Sweep>57.000000</Sweep>
    <SweepLoc>0.000000</SweepLoc>
    <Twist>0.000000</Twist>
  </Section>
</Section_List>
  
```

```

<Span>2.013295</Span>
<TC>1.685525</TC>
<RC>2.923869</RC>
<Sweep>57.000000</Sweep>
<SweepLoc>0.000000</SweepLoc>
<Twist>0.000000</Twist>
<TwistLoc>0.000000</TwistLoc>
<Dihedral>0.000000</Dihedral>
<Dihed_Crv1>0.000000</Dihed_Crv1>
<Dihed_Crv2>0.000000</Dihed_Crv2>
<Dihed_Crv1_Str>0.750000</Dihed_Crv1_Str>
<Dihed_Crv2_Str>0.750000</Dihed_Crv2_Str>
<DihedRotFlag>0</DihedRotFlag>
<SmoothBlendFlag>0</SmoothBlendFlag>
<NumInterpXsecs>1</NumInterpXsecs>
    
```

Fig. 6 Data structure from OpenVSP. The parameter for the cant angle is highlighted in red, and the parameter for the sweep angle is highlighted in green.

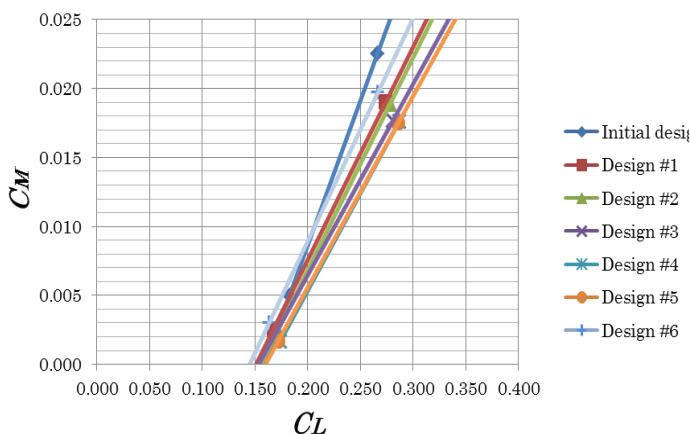
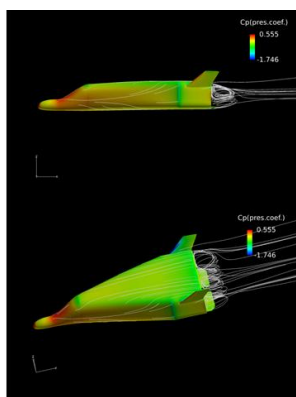
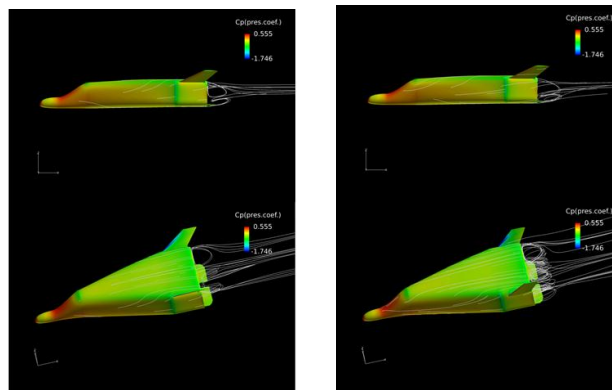


Fig. 7 Comparison of C_L - C_M relationship among sample designs and the initial design.



(a) Initial design



(b) Design #4.

(c) Design #5.

Fig. 8 Comparisons of the flowfield among the initial design, designs #4 and #5.

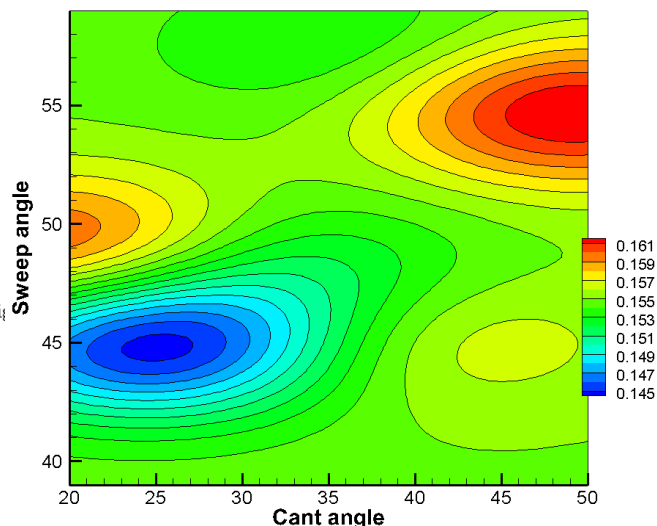


Fig. 9 Visualization of design problem by means of Kriging surrogate model.

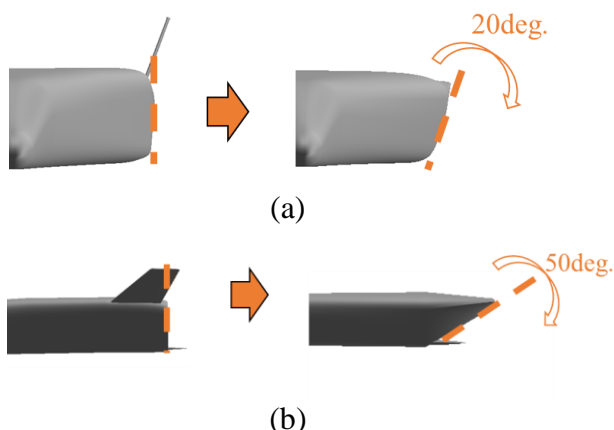
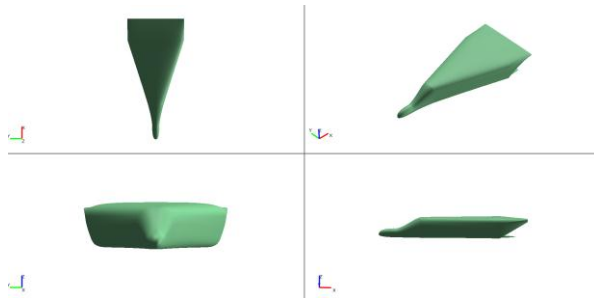


Fig. 10 Modification of the fuselage for removal of the V-tail.

DEVELOPMENT OF AERODYNAMIC DESIGN PROCESS FOR REUSABLE WINGED SPACE VEHICLE USING OPENVSP



(a) Design A

Fig. 11 Three-views of the modified design. This design does not have V-tail and the aft shape is modified for the trim balance

5 Conclusions

The aim of this paper is the proposal of an efficient design procedure using OpenVSP and the demonstration of the design of a winged spacecraft. First, a rapid global geometry design procedure is developed using OpenVSP and a high-fidelity flow solver. Then, this procedure is applied to the winged space craft whose original concept was provided by JAXA as a lifting body. This study considers the lift maximization at the landing condition, with the variation of the cant angle and the sweep angle of the vertical tail (V-tail). In conclusion:

- The proposed procedure is an efficient tool for geometrical design.
- Considering the lift maximization at the trim balanced condition, two kinds of V-tail design are acquired. One is with a large cant angle, and the other is with a low cant angle.
- Each optimum design has a similar sweep angle, $50\text{--}55^\circ$. A large sweep back angle is appropriate for the landing condition of the spacecraft.
- According to the design visualization result, the low cant angle has possibility to achieve better performance. This result suggests that topological optimization including the possibility of V-tail removal may find a better design. If the V-tail could be removed, such a design should show good heat-resistance, and maintain the lift and the trim balance by optimization of the body.

- The proposed design procedure based on OpenVSP has the possibility to be an efficient design tool which can discover the design knowledge regarding the geometry and the topology at a same time.

Acknowledgement

I would like to thank my thesis advisors, associate professor Masahiro Kanazaki in Tokyo Metropolitan University for his guidance, support. I wish to thank Dr. Takashi Aoyama, Dr. Atsushi Hashimoto, Dr. Takashi Ishida in Aerospace Research and Development Directorate of Japan Aerospace Exploration Agency for providing me the computational codes, the account of the supercomputer and useful advices for my research. I also wish to thank Dr. Shinji Ishimoto and Dr. Yoshinori Minami in Space Transportation Mission Directorate of Japan Aerospace Exploration Agency for providing me the geometric data of the spacecraft and the account of super computer for my research.

References

- [1] <http://www.openvsp.org/>
- [2] P. R. Lahur, "Automatic Hexahedra Grid Generation Method for Component-based Surface Geometry" 17th AIAA Computational Fluid Dynamics Conference, 2005.
- [3] Hashimoto, A., et al., "DEVELOPMENT OF FAST UNSTRUCTURED CFD CODE "FASTAR"," Proceedings of ICAS2012, 2012.
- [4] Y. Nakayama, M. Kanazaki, Y. Fukuyama, M. Murayama, and K. Yamamoto, "Design of Novel Wing Body Considering Intake/ Exhaust Effects," APISAT 2013.
- [5] K. Fujii, S. Ishimoto, T. Mugitani, and Y. Minami, "Present Status and Prospects of JAXA's Research on Future Space Transportation System," AIAA-2012-5849, 2012.
- [6] T. Tanaka, N. Sakamoto, and K. Koyamada, "Hierarchical Response Surface Methodology," Journal of Japan Society for Simulation Technology, Vol. 2, No. 1, pp.22-31, 2010 (written in Japanese).

Copyright Statement

The authors confirm that they, and/or their company or organization, hold copyright on all of the original material included in this paper. The authors also confirm that they have obtained permission, from the copyright holder of any third party material included in this paper, to publish it as part of their paper. The authors confirm that they give permission, or have obtained permission from the copyright holder of this paper, for the publication and distribution of this paper as part of the ICAS 2014 proceedings or as individual off-prints from the proceedings.